Parameter optimization and experiment of the vacuum seed meter with double holes for direct seeding of rice

Cheng Qian[1,2], Wei Qin[1,2*], Youcong Jiang[1,2], Zishun Huang[1,2], Minghua Zhang[1,2,3,4], Zaiman Wang[1,2,3,4], Wenwu Yang[1,2,3,4], Ying Zang[1,2,3,4*]

(1. *College of Engineering, South China Agricultural University, Guangzhou 510642, China*;
2. *China Key Laboratory of Key Technology on Agricultural Machine and Equipment (South China Agricultural University), Ministry of Education, Guangzhou 510642, China*;
3. *State Key Laboratory of Agricultural Equipment Technology, Beijing 100083, China*;
4. *Huangpu Institute of Innovation, South China Agricultural University, Guangzhou 510642, China*)

Abstract: Direct seeding of rice is a green planting technique because it reduces irrigation water and lowers agricultural production costs. A vacuum seed meter with a double hole for rice was developed to improve the planting accuracy of direct seeding and to meet the tiny seeding rate. The key components of the vacuum seed meter were theoretically analyzed and designed. The optimal parameters of the seed disturbance structure were determined by the Box-Behnken test using the quality of feed index (each group of holes is 1 to 2), miss index, and multiple index as test indices. The results of the Box-Behnken test showed that the optimal parameters were a height of the seed disturbance structure of 1.65 mm, a diameter of the upper arc of 98.87 mm, and a central angle of the upper arc of 11.4°. Based on the optimal seed disturbance structure, the effect of the shaped hole structure parameters on the planting accuracy was investigated, and the optimal hole width and depth were determined to be 4 mm and 2 mm. CFD-DEM numerical simulations showed that the pressure gradient force on the seeds was greater than the drag force, and the pressure gradient force and drag force were positively correlated with the width of the shaped hole. When the rotational speed was 60 r/min and the vacuum pressure was 2.0 kPa, 2.4 kPa, and 2.8 kPa, the miss index of the vacuum seed meter with Wuyou 1179 as the test material was 3.52%, 2.5%, and 2.22%; the quality of feed index was 92.41%, 92.13%, and 87.13%; and the multiple index was 4.07%, 5.37%, and 10.65%. For Huanghuazhan and Taixiang 812 rice seeds, the planting accuracy of the vacuum seed meter with the double hole can meet the requirements for direct seeding of rice. This study provides a theoretical basis and design reference for rice precision planting technology.

Keywords: rice, direct seeding, seed meter, planting accuracy, shaped hole, seed disturbance structure, CFD-DEM
DOI: 10.25165/j.ijabe.20251802.9335

Citation: Qian C, Qin W, Jiang Y C, Huang Z S, Zhang M H, Wang Z M, et al. Parameter optimization and experiment of the vacuum seed meter with double holes for direct seeding of rice. Int J Agric & Biol Eng, 2025; 18(2): 89–99.

1 Introduction

Rice is widely grown worldwide and is one of the most essential food crops[1,2]. Direct seeding of rice is the direct sowing of rice seeds into paddy fields or drylands[3,4]. Compared to transplanting, rice direct seeding eliminates the process of seedling cultivation[5,6]. It also reduces production costs for labor and equipment. Traditional rice transplanting methods use much water, two to three times more than other grain crops such as corn or wheat[7,8]. The irrigation water used for direct seeding of rice is less than that for transplanting. Some studies have shown that direct seeding of rice has a well-developed root system and is lodging-resistant, and the yield of direct seeding of rice is close to that of transplanted rice[9,10]. Rice direct seeding can be divided into manual seeding and mechanical direct seeding. Mechanical direct seeding of rice allows for an orderly distribution of rice, facilitating field management and growth uniformity[11,12]. The rice direct seeding planter mainly adopts mechanical seed metering devices, and its seeding volume is larger to ensure the emergence rate in the field. With advances in breeding technology, the emergence rate of rice has increased, so costs can be reduced by reducing the amount of rice seed in the field. Vacuum seed meters have the advantages of low damage, high planting precision, and seed saving[13-16]. However, due to the low sphericity of rice seeds and high inter-seed friction, the rice vacuum seed meter suffers from low seed-filling rate, fluctuating planting precision, and easy clogging of suction holes.

Vacuum seed metering systems, such as cotton, peanut, corn, and soybean, are mainly used for precision planting[17,18]. The method of positive pressure air flow and inclined seed disc is used to improve the seed falling speed of the seed meter, and the research proves that the high-speed positive pressure air flow can improve the uniformity of seed spacing[19]. The maize seed meter with a double air chamber was designed to meet the agronomic requirements of two rows on a ridge[20]. The effects of different seed

Received date: 2024-08-30 **Accepted date:** 2025-02-18
Biographies: Cheng Qian, PhD candidate, research interest: agricultural mechanization and automation, Email: chengqian@stu.scau.edu.cn; **Youcong Jiang**, PhD candidate, research interest: agricultural mechanization and automation, Email: jiangyc@stu.scau.edu.cn; **Zishun Huang**, PhD candidate, research interest: agricultural mechanization and automation, Email: huangzs@stu.scau.edu.cn; **Minghua Zhang**, Associate Professor, research interest: agricultural mechanization and automation, Email: zhangminghuascau@163.com; **Zaiman Wang**, Professor, research interest: agricultural mechanization and automation, Email: wangzaiman@scau.edu.cn; **Wenwu Yang**, Associate Professor, research interest: agricultural mechanization and automation, Email: yangwenwu@scau.edu.cn.
***Corresponding author: Wei Qin**, PhD, research interest: agricultural mechanization and automation, Email: qinweilxy@scau.edu.cn; **Ying Zang**, PhD, Professor, research interest: agricultural mechanization and automation. College of Engineering, South China Agricultural University, Guangzhou 510642, China. Tel: +86-20-38676975, Email: yingzang@scau.edu.cn.

postures on the quality of feed index, miss index, and multiple index were investigated. The horizontal seed posture was conducive to improving the planting accuracy of the maize seed meter. A high-speed metering system with rotating impellers for seed separation has been developed, and the influence of the structural parameters of the seed delivery system on seeding accuracy was analyzed using high-speed photography[21]. A centrifugal filling and cleaning seed meter for operating speeds of 10-20 km/h was designed, and tests have shown that only 10.94 W of power is required at the highest operating speed of the seed meter[22]. Based on the sunflower shape fitting equation, a shape-hole vacuum seed meter for sunflowers was designed, and the experiment proved that the shape-hole structure improved the planting accuracy of the meter[23]. A seed meter with left and right discs was invented for high-density planting, where the left disc is seeded, followed by the right disc, and then alternated in that order[24]. A study was carried out on the effect of different numbers of seed suction holes on the quality of feed index, multiple index, miss index, and seed spacing uniformity using a computerized measurement system[25]. With the development of artificial intelligence technology, it has become possible to build a predictive model for planting accuracy using an artificial neural network method. Models were established for the surface area, thousand kernel weight, density, sphericity, and the optimum vacuum of soya bean, maize, and sugar beet crops by the Levenberg-Marquardt learning algorithm[26]. Based on an artificial neural network and multi-objective particle swarm optimization, a prediction model of the quality of feed index was established, and the structural parameters of the seed meter under the optimal quality of feed index were determined[27]. Computational fluid dynamics (CFD) and discrete element methods (DEM) can be used to analyze fluid-particle interactions. In engineering applications, CFD-DEM coupling is widely used in pneumatic conveying[28], the fluidized bed[29], and the mining industry[30]. Of course, agricultural engineering has also seen the application of discrete element methods and computational fluid dynamics. A numerical simulation of the working process of the vegetable seed meter was carried out by CFD-DEM coupling to determine the key structural parameters of the meter[31]. A numerical simulation of the distribution system of a seed drill was conducted to study the effects of the structural parameters of the distribution system on the seed and airflow and optimize the distribution system[32].

Currently, the main focus of research on seed meters is on seeds with high sphericity and large size. Rice has more pubescence on its surface compared to other crops such as maize or wheat. On the one hand, coarse pubescence reduces the mobility of the rice seeds in the seed chamber so that the suction holes do not easily absorb the seeds. On the other hand, pubescence increases the population action on the adsorbed seeds, causing the adsorbed seeds to detach from the suction holes. As the disc rotates, some pubescence or broken glumes fall off the rice seeds and enter the suction holes under vacuum pressure, clogging the suction holes. Large-particle seeds are typically cleaned from the suction holes of the seed meter with a seed unloading wheel, while small-particle seeds are cleaned from the suction holes with a positive airflow. The small diameter of the rice suction holes precludes the use of a seed unloading wheel structure. Rice suction holes can become clogged with broken seeds, and relying on positive pressure airflow will not clear the holes. The general vacuum seed meter has a single-hole structure, while the vacuum seed meter for rice has a double hole in each group to ensure emergence in the field. Therefore, the vacuum seed meter with the double hole for rice was optimized for 1 to 2 seeds per group of suction holes.

A vacuum seed meter with the double hole for direct seeding of rice is proposed in this study. Key components of the vacuum seed meter were designed and analyzed. Tests were conducted to determine the optimal parameters for the seed disturbance structure. Based on the optimal seed disturbance structure, the effects of the structural parameters of the shaped hole on the quality of feed index, miss index, and multiple index were investigated. The CFD-DEM coupling method was used to simulate the working process of the seed meter and to analyze the effect of different shaped holes on suctioning rice seed. This study can provide a reference for rice precision direct seeding technology.

2 Materials and methods

2.1 Design of key components of the seed meter

2.1.1 Structure and working principle of the seed meter

The main structure of the vacuum seed meter with the double hole for rice is shown in Figure 1, including the seed inlet, seed chamber, seed guard ring, disc, isolating brush, anti-clogging brush, and air chamber. The seed guard ring is located between the seed chamber and the disc and prevents the seed from falling into the gap between the seed chamber and the disc. The seeds in the seed chamber flow around the shaped holes under the action of the disturbed seed structure of the disc, and the seeds are adsorbed by the shaped holes under vacuum pressure. The shaped holes increase the friction between the rice seed and the disc, which can reduce the action of seeds on the suctioned seed to prevent the suctioned seed from moving from the hole. The suctioned seeds rotate with the disc to the seed-throwing area, where the seeds are removed from the holes by centrifugal inertia force and gravity. The foreign matter in the hole is removed by the clogging device and the isolating brush, avoiding the reduction of planting accuracy due to clogged suction holes.

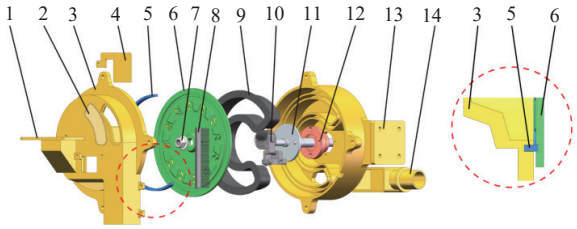

1. Seed inlet 2. Transparent window 3. Seed chamber 4. Seed feed adjustment plate 5. Seed guard ring 6. Disc 7. Fixing nut 8. Isolating brush 9. Sealing rubber 10. Anti-clogging device 11. Shaft 12. Bearing 13. Air chamber 14. Vacuum port

Figure 1 Vacuum seed meter with double hole for rice

2.1.2 Number of suction hole groups

The number of suction hole groups in the seed meter affects the frequency of throwing seeds at the same speed. Therefore, the number of suction hole groups in the rice vacuum seed meter must be determined based on the agronomic requirements and operating parameters. The time interval between two seedings can be found according to Equation (1):

$$\Delta t = \frac{S}{v_m} = \frac{2\pi}{N\omega} \tag{1}$$

where, Δt is the time interval between two seedings, s; S is the seed spacing for rice direct-seeding, m; v_m is the forward speed of the planter, m/s; N is the number of suction hole groups; ω is the angular velocity of the seed, rad/s.

According to Equation (1), the number of suction hole groups N can be obtained according to Equation (2):

$$N = \frac{2\pi v_m}{S\omega} = \frac{60 v_m}{S n} \tag{2}$$

where, n is the rotation speed of the seed meter, r/min.

The seed spacing for rice direct-seeding is 0.1-0.2 m. The paddy field tractor is used to power the rice precision direct-seeding planter. The field operating speed of the paddy field tractor is typically 0-1.3 m/s. For the calculation, the forward speed of the planter is assumed to be 1.3 m/s. The working rotation speed of the seed meter shaft of the rice precision planter is generally 30 to 60 r/min. According to Equation (2), the number of suction hole groups of the seed meter can be obtained from 7.5 to 26. Due to the double-hole structure, an excessive number of suction holes can cause geometric interference, and the final number of suction holes is 12.

2.1.3 Shaped hole structure

The triaxial dimensions of three rice varieties were measured to provide a design basis for determining the hole diameter and the structural parameters of the shaped hole. The measurements were made using calipers with an accuracy of 0.01 mm, the sample size was 100 grains, and the triaxial dimensions of rice were obtained, as listed in Table 1.

Table 1 The triaxial dimensions of rice seeds

Variety	L_{avg}/ mm	W_{avg}/ mm	T_{avg}/ mm	L_{max}/ mm	W_{max}/ mm	T_{max}/ mm	L_{min}/ mm	W_{min}/ mm	T_{min}/ mm
Wuyou 1179	8.49	2.43	1.85	9.72	2.98	2.31	6.4	1.83	1.34
Huanghuazhan	9.44	2.16	1.88	10.59	2.53	2.2	8.22	1.84	1.64
Taixiang 812	10.62	1.93	1.72	11.79	2.23	1.98	9.3	1.67	1.43

The mechanical analysis of the instantaneous critical state during seed filling of the seed meter disc without shaped holes and the force analysis of seed filling of the meter without shaped holes are shown in Figure 2. The forces of the disc without shaped holes in three directions were obtained, as shown in Equation (3):

$$\begin{cases} Z: f_{D1}\sin\theta = G + J\cos\theta + F_{P1}\sin\theta \\ X: F_{P1}\cos\theta = J\sin\theta + f_{D1}\cos\theta \\ Y: F_{N1} = F_{S1} + F_{V1} \end{cases} \tag{3}$$

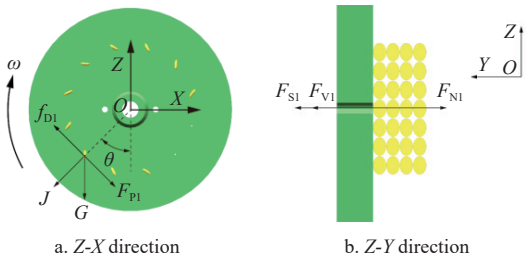

a. *Z*-*X* direction b. *Z*-*Y* direction

Note: f_{D1} is the frictional force between the disc without the shaped hole and the seeds, N; G is the gravity of the seeds, N; J is the centrifugal inertia force, N; F_{P1} is the action force by seeds of the disc without the shaped hole on the suctioned seed, N; F_{N1} is the support force of the disc without the shaped hole on the seed, N; F_{S1} is the suction force of the hole on the seeds, N; F_{V1} is the squeezing force by seeds of the disc without the shaped hole on the suctioned seed, N; θ is the angle between the line connecting the hole and the center of the disc without the shaped hole and the direction of the *Z*-axis, (°).

Figure 2 Force analysis of seed disc without the shaped hole structure

Then, the mechanical analysis of the instantaneous critical state during seed filling of the shaped hole was carried out, and the seed-filling force analysis of the shaped hole structure is shown in Figure 3. The forces of the disc with shaped holes in three directions were obtained, as shown in Equation (4).

It can be seen that the seeds suctioned on the disc with the shaped hole have more friction between the two sides of the shaped hole compared to the seeds on the disc without the shaped hole, combining Equation (3) and Equation (4). When the gravity of the seed and the centrifugal inertia force are equal, the suction force required for the seed meter with the shaped hole is smaller, and the seed-filling performance of the seed meter can be improved by adopting the shaped hole structure.

$$\begin{cases} Z: f_{D2}\sin\alpha + f_H\cos\beta = G + J\cos\alpha + F_{P2}\sin\alpha \\ X: F_{D2}\cos\alpha = f_{P2}\cos\alpha + f_H\sin\beta + J\sin\alpha \\ Y: F_{N2} = F_{S2} + F_{V2} \end{cases} \tag{4}$$

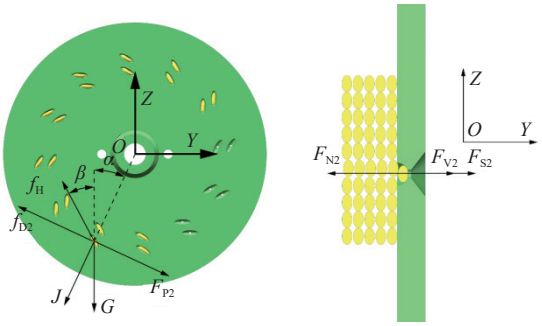

a. *Z*-*X* direction b. *Z*-*Y* direction

Note: f_{D2} is the frictional force between the disc with the shaped hole and the seeds, N; f_H is the friction force between the two sides of the shaped hole and the seed, N; F_{P2} is the action force by seeds of the disc with the shaped hole on the suctioned seed, N; F_{N2} is the support force of the disc with the shaped hole on the seed, N; F_{S2} is the suction force of the shaped hole on the seeds, N; F_{V2} is the squeezing force by seeds of the disc with the shaped hole on the suctioned seed, N; α is the angle between the line connecting the hole and the center of the disc with the shaped hole and the direction of the *Z*-axis, (°); β is the angle between f_H and the direction of the *Z*-axis, (°).

Figure 3 Force analysis of seed disc with the shaped hole structure

The seed meter's shaped hole structure should match the seed's shape, so the vacuum seed meter with the double hole for rice adopts a spindle-shaped hole structure. The shaped hole structure is shown in Figure 4, and the structural parameters can be calculated according to Equation (5). According to Equation (5) and Table 1, the length of the shaped hole L_m is 11.79-12.8 mm, the width of the shaped hole W_m is 2.98-6.4 mm, and the thickness of the shaped hole T_m is 1.49-3.2 mm. Subsequent tests determined the width and the thickness of the shaped hole.

$$\begin{cases} L_{max} < L_m < 2L_{min} \\ W_{max} < W_m < L_{min} \\ T_m = \dfrac{W_m}{2} \end{cases} \tag{5}$$

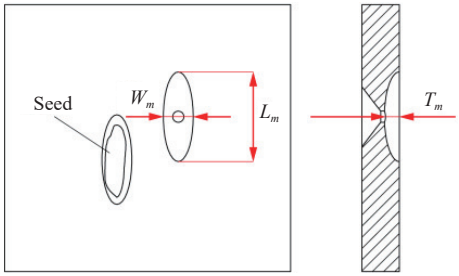

Figure 4 Shaped hole structure of vacuum seed meter

2.1.4 Hole diameter

Assuming that the cross-section of the airflow at a distance x from the center of the suction hole is a sphere (Figure 5), that the velocities on the cross-section are equal, and that the gas flow rate through the cross-section is equal to the gas flow rate through the seed suction hole, the arbitrary velocity v_x on the spherical cross-section is calculated according to Equation (6):

$$v_x = \frac{Q}{A_x} = \frac{\pi d_h^2 v_h}{4A_x} \tag{6}$$

where, Q is the gas flow rate through the suction hole cross-section, m³/s; A_x is the gas flow cross-section area at the center x of the suction hole, m²; d_h is the diameter of the suction hole, m; v_h is the flow rate in the suction hole, m/s².

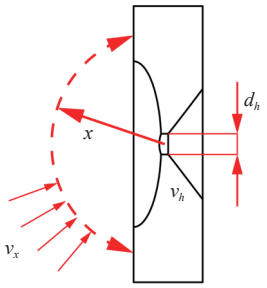

Figure 5 Velocity analysis of suction hole structure

According to the fluid mechanics principle, the particle's drag force F_D in the flow field can be calculated using Equation (7):

$$F_D = \frac{1}{2} C_D A_P \rho (v - v_p) \tag{7}$$

where, C_D is the drag coefficient; A_p is the windward area, m²; ρ is the flow density, kg/m³; v is the flow velocity, m/s; v_p is the particle velocity, m/s.

Simultaneous Equations (6) and (7), which gives

$$F_D = \frac{1}{2} C_D A_P \rho \frac{\pi d_h^2 v_h}{4A_X} \tag{8}$$

From Equation (8), it can be seen that when the flow velocity v_h in the suction hole is constant, the drag force increases when the diameter of the suction hole increases. If the width of the rice is larger than the thickness, and the diameter of the hole is smaller than the minimum rice width, the seed can be prevented from being suctioned into the inside of the air chamber through the hole. From Table 1, the minimum rice width is 1.67 mm, so the suction hole diameter is assumed to be 1.6 mm.

2.1.5 Suction hole position

The air chamber structure of the seed meter is shown in Figure 6, where D_1 and D_2 are 110 mm and 160 mm, respectively, so that the center of the flow field is positioned at a diameter of 135 mm. The holes are oriented in the Z direction (Figure 7) to ensure the seeds fall vertically. Each group of holes of the vacuum rice seed meter has two suction holes, and the relative positions of the two suction holes need to be determined. The kinetic analysis diagram is shown in Figure 7. The circumferential velocity of the inner suction hole and the circumferential velocity of the outer suction hole are given by Equations (9) and (10), respectively.

$$v_{P1} = \omega R_1 \tag{9}$$

$$v_{P2} = \omega R_2 \tag{10}$$

The distance between the inner and outer holes to the soil surface when throwing seeds is shown in Equations (11) and (12):

$$H_1 = t_1 v_{P1} \cos\gamma + \frac{1}{2} a_1 t_1^2 \tag{11}$$

where, t_1 is the time for the seeds with the inner hole to complete the seed-throwing process, s; a_1 is the acceleration of the seeds with the inner hole in the seed-throwing process, m/s².

$$H_2 = t_2 v_{P2} \cos\gamma + \frac{1}{2} a_2 t_2^2 \tag{12}$$

where, t_2 is the time for the seeds with the inner hole to complete the seed-throwing process, s; a_2 is the acceleration of the seeds with the inner hole in the seed-throwing process, m/s².

From Figure 7, it can be seen that there are geometric relationships as shown in Equations (13) and (14):

$$H_2 = H_1 + H \tag{13}$$

$$H = (R_2 - R_1)\sin\lambda \tag{14}$$

If the inner seeds fall to the soil at the same time as the outer seeds, according to Equations (9) to (14), the time for the seed throwing process t can be obtained (Equation (15)):

$$t = \frac{\sqrt{\omega^2 R_1^2 \cos^2\gamma + 2a_1 H_1} - \omega R_1 \cos\gamma}{a_1} = \frac{\sqrt{\omega^2 R_2^2 \cos^2\gamma + 2a_2 (H_1 + (R_2 - R_1)\sin\lambda)} - \omega R_2 \cos\gamma}{a_2} \tag{15}$$

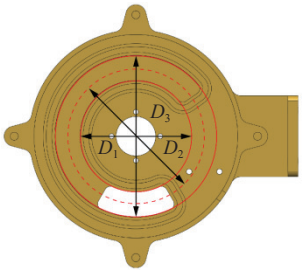

Figure 6 Air chamber of vacuum seed meter with double hole for rice

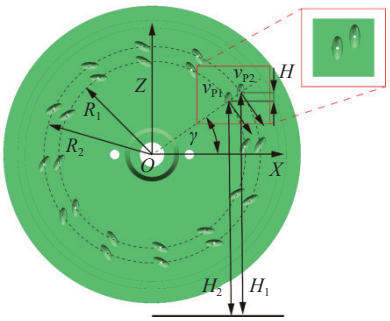

Note: R_1 is the radius of the inner hole position, m; R_2 is the radius of the outer hole position, m; H_1 is the distance between the inner hole to the soil surface when throwing seeds, m; H_2 is the distance between the outer hole to the soil surface when throwing seeds, m; H is the distance between the outer suction hole and inner suction hole in the Z-direction; v_{P1} is the circumferential speed of the inner hole, m/s; v_{P2} is the circumferential speed of the outer hole, m/s; γ is the angle between the line connecting the center of the disc and the hole and the X-direction when throwing seeds, (°).

Figure 7 Schematic diagram of the kinematic analysis of the seed-throwing process

As seen from Equation (15), the height of the seed on the outer holes should be higher than the seeds on the inner holes when they achieve synchronous throwing. A series of conditions must be satisfied if the time for the seeds on both sides of the hole to

complete the seed-throwing process is the same. However, there will be a difference in the acceleration of the seeds on both sides due to the different falling attitudes during seed throwing. The speed of the seed meter must also be adjusted according to the agronomic requirements. It is difficult to ensure that the seeds on both sides fall simultaneously in the actual seeding process, and the distance between R_1 and R_2 can only be reduced to shorten the landing time interval. The center of the two suction holes and the center of the seed meter should be in the same straight line to ensure that the seeds fall simultaneously. Seeds on both sides should be distributed near the center of the flow field using R_1 as 62.5 mm, R_2 as 72.5 mm, and γ as 35°.

2.1.6 Seed disturbance structure

The poor fluidity of rice seeds is not conducive to the suction of rice seeds by the seed meter. A seed disturbance structure was designed to improve seed fluidity inside the seed meter (Figure 8). The holes are located between the two seed disturbance structures. As the seed disc rotates, the seed flows from the top arc of the seed disturbance structure to the bottom arc to improve the seed-filling performance of the seed meter. To avoid interference between the seed disturbance structure and the hole structure, the diameter of the lower arc was first determined to be 155 mm, and the central angle of the lower arc was determined to be 20°. The upper arc diameter D_1, the upper arc central angle φ, and the seed disturbance structure height h were determined by subsequent Box-Behnken tests. The height h of the seed disturbance structure is 0.5-2.5 mm, the diameter of the upper arc is 85-115 mm, and the central angle of the upper arc is 6°-18°.

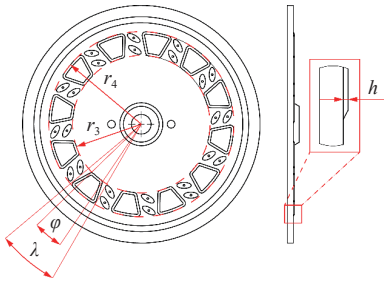

Note: R_3 is the diameter of the upper arc, mm; R_4 is the diameter of the lower arc, mm; φ is the central angle of the upper arc, (°); λ is the central angle of the lower arc, (°); h is the height of the disturbance structure, mm.

Figure 8 Seed disturbance structure of vacuum seed meter

2.1.7 Design of anti-clogging device

The flow of rice seeds inside the seed chamber can cause an increase in pubescence or broken glumes due to interactions between seeds or between seeds and the disc, which can result in clogging of the suction holes. Clogging of the suction hole will reduce the seed-filling performance of the seeder, and in severe cases, misses will occur, reducing the planting accuracy. An anti-clogging device was designed to prevent clogging of the suction holes (Figure 9), which mainly consists of the base, articulated shaft Ⅰ, spring, brush roller, bracket, and articulated shaft Ⅱ. Friction occurs between the brush roller and the back of the disc under the action of the spring support force. As the disc rotates, the brush roller rotates due to friction. The brush roller can clean the foreign matter in the suction hole to prevent the suction hole from clogging. The isolating brush can clean the front of the disc because the suction holes pass through the isolation brushes. The back of the disc has a groove structure, which makes it easy for the anti-clogging device to clean the suction hole of foreign matter. In subsequent tests, the spring parameters need to be determined.

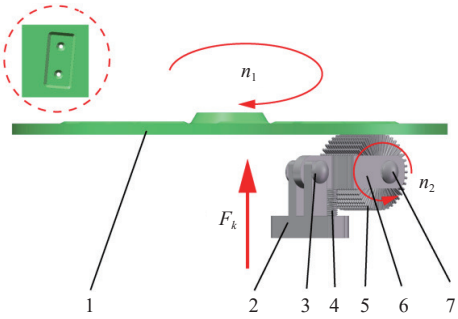

Note: F_k is the support force of the spring on the bracket, N; n_1 is the speed of the disc, r/min; n_2 is the brush roller, r/min.

1. Seed disc 2. Base 3. Articulated shaft Ⅰ 4. Spring 5. Brush roller 6. Bracket 7. Articulated shaft Ⅱ

Figure 9 Anti-clogging device of seed meter

2.2 Experimental design

2.2.1 Anti-clogging device

The spring of the anti-blocking device allows the brush roller to interact with the disc of the seed meter. A high spring force can increase friction, and a low spring force will result in a small contact area between the brush roller and the disc. The structural parameters of the spring include outside diameter×length×wire diameter. From the structure of the anti-blocking device, it can be determined that the outer diameter and length are 6 mm and 20 mm, respectively, and the wire diameter of the spring must be determined. The rotation speed of the seed meter must be measured after installing springs of different wire diameters to determine the structural parameters of the springs.

2.2.2 Seed disturbance structure

A Box-Behnken test with 17 trials was conducted to determine the parameters of the optimal seed disturbance structure, using the height of the seed disturbance structure, the diameter of the upper arc, and the central angle of the upper arc as test factors, and quality of feed index, miss index, and multiple index of the seeds of Wuyou 1179 as test indices. For the test, the shaped hole width W_m and shaped hole thickness T_m were assumed to be 4 mm and 2 mm, respectively. In order to make the effect of the seed disturbance structure on the seeding accuracy more significant, it is necessary to choose a low vacuum pressure and a common rotational speed, so the vacuum pressure and rotational speed were assumed to be 2.0 kPa and 40 r/min, respectively. The factors and levels of the test are listed in Table 2. 3D printing was used to fabricate seed discs with different seed disturbance structures (Figure 10), and the material was high-strength resin.

Table 2 Factors and levels of Box-Behnken test

Level code	Factor		
	Height/mm	Diameter of upper arc/mm	Central angle of upper arc/(°)
1	2.5	115	18
0	1.5	100	12
–1	0.5	85	6

2.2.3 Shaped hole structure

(1) Physical experiment

Based on the optimal seed disturbance structure, four seed discs with different shaped hole structure parameters were designed and 3D printed with shaped hole widths W_m of 3 mm, 4 mm, 5 mm, and 6 mm, and shaped hole thicknesses T_m of 1.5 mm, 2 mm, 2.5 mm, and 3 mm (Figure 11). Tests were conducted to determine the quality of feed index, miss index, and multiple index of Wuyou 1179 seeds at speeds of 20 r/min, 40 r/min, and 60 r/min, and vacuum pressures of 1.6 kPa, 2.0 kPa, 2.4 kPa, 2.8 kPa, and 3.2 kPa.

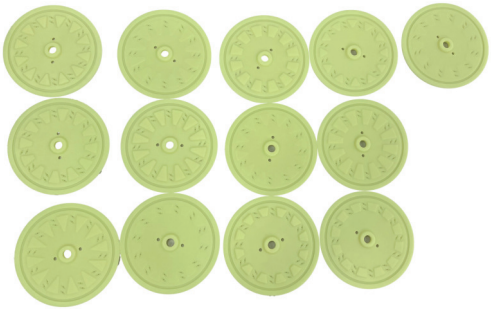

Figure 10 Disc of seed meter with seed disturbance structure

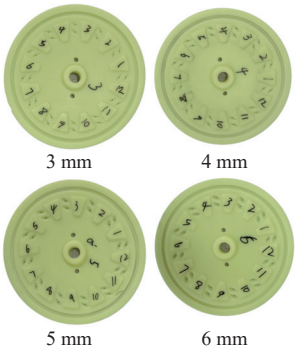

Figure 11 Seed discs with different shaped hole structure parameters

(2) CFD-DEM numerical simulations

In order to thoroughly analyze the influence of shaped hole structure parameters on rice seed suction, a numerical simulation of the working process of the seed meter was carried out by a two-way coupled CFD-DEM method. The two-way CFD-DEM coupling uses a semi-resolved method for larger particle sizes than the fluid mesh. The Haider and Levenspiel model for non-spherical particles was used for the drag model. The fluid domain was solved using Ansys Fluent 2024, and the discrete domain was solved using Ansys Rocky 2024, and both exchanged data after the unit time step calculation was completed (Figure 12).

The fluid domain of the seed meter consists of the seed chamber, the shaped hole, and the air chamber, and an SST k-ω turbulence model was used for the calculations. A mesh motion was used to simulate the moving shaped hole fluid domain, creating interface A between the seed chamber and the shaped hole, and interface B between the shaped hole and the air chamber. Local refinement of the interfaces is used to improve the accuracy of the numerical simulations. A discrete element model of rice seed was developed with the physical parameters of Wuyou 1179 rice seed. The Poisson's ratios of rice seed and seed meter were 0.25 and 0.42, the densities were 1045 kg/m^3 and 1120 kg/m^3, and the shear moduli were 108 MPa and 2700 MPa, respectively. The restitution coefficient, static friction, and dynamic friction between rice seeds were 0.25, 0.5, and 0.01, respectively. The restitution coefficient, static friction, and dynamic friction between rice seeds and seed meter were 0.52, 0.48, and 0.01, respectively. The simulation was performed with a seed disc speed of 40 r/min, a vacuum of 2800 kPa, and a simulation time of 3 s.

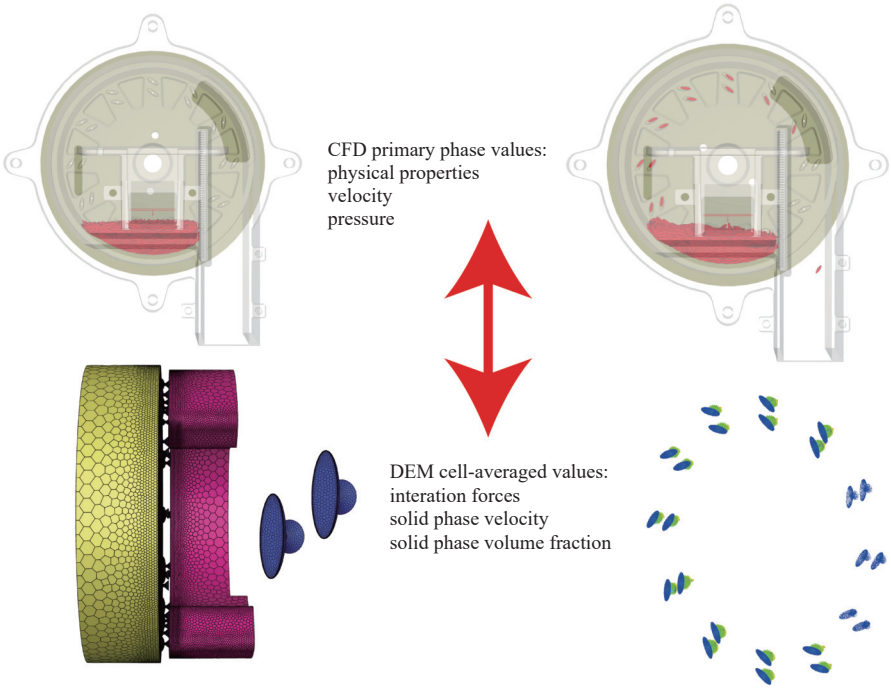

Figure 12 Principle of CFD-DEM coupling for seed meter

2.3 Test equipment and materials

2.3.1 Test bench

The seed meter test stand, shown in Figure 13, consists mainly of the motor, motor speed governor, air pressure sensor, hall sensor, fan, fan speed governor, and seed meter. A motor governor controls the rotation speed of the seed meter with an accuracy of ±1 r/min. A fan speed governor controls the vacuum pressure of the seed meter with an accuracy of ±0.05 kPa. The hall and air pressure sensors primarily measure the seed meter's speed and vacuum, making it easy to adjust the speed and vacuum pressure accurately. A mobile phone was used to film the operation of the seed meter in slow motion. Based on the video, the number of seeds suctioned by each group of holes of the seed meter was manually counted.

2.3.2 Rice seed

Seeds from Wuyou 1179, Huanghuazhan, and Taixiang 812 were selected for the experiment (Figure 14), with an average moisture content of <13%. The average length, width, and thickness are 8.49 mm, 2.43 mm, and 1.85 mm for Wuyou 1179; 9.44 mm, 2.16 mm, and 1.88 mm for Huanghuazhan; and 10.62 mm, 1.93 mm, and 1.72 mm for Taixiang 812. The thousand-grain weight of

Wuyou 1179 is 23.5-3.7 g, that of Huanghuazhan is 22.2-23.1 g, and that of Taixiang 812 is 19.2-19.3 g.

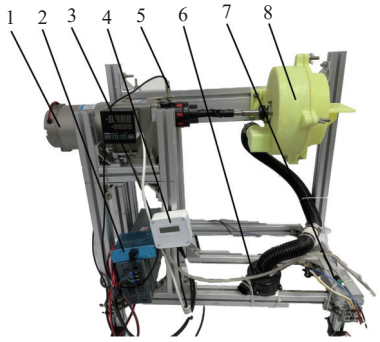

1. Motor 2. Motor speed governor 3. Display of rotation speed 4. Display of vacuum pressure 5. Hall sensor 6. Fan 7. Fan speed governor 8. Seed meter

Figure 13 Test bench of the seed meter

Figure 14 Rice seeds used in tests

3 Results and discussion

3.1 Anti-clogging device

The test results are shown in Figure 15. As the spring wire diameter increases, the friction between the brush roller and the disc increases, resulting in a decrease in speed. The spring parameters are selected to be 20 mm×6 mm×0.6 mm to minimize the influence of the brush roller on the disc and ensure that the anti-clogging device has sufficient spring force. The internal structure of the seed meter after 4 hours of operation is shown in Figure 16, which shows that the suction holes are not clogged and there is some dirt on the brush roller. The anti-clogging device can effectively remove the dirt on the suction hole and prevent the suction hole from clogging.

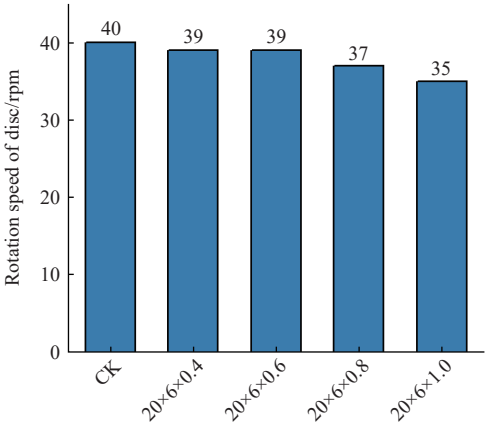

Note: CK is without spring.

Figure 15 Variation of rotation disc speed for different spring parameters

3.2 Seed disturbance structure

The results of the Box-Behnken test are shown in Table 3, and regression models were established based on test results. The variance analysis is listed in Table 4 (the regression model for multiple index was insignificant). The results indicated that the regression model for quality of feed index was highly significant, with the effect of the quadratic form x_1^2 on quality of feed being highly significant, and the effects of the primary form x_1, the quadratic form x_2^2, and the quadratic form x_3^2 on quality of feed being significant. The regression model for the miss index was significant, with the effect of the quadratic form x_1^2 on the miss index being highly significant, and the effect of the primary form x_1 on the miss index being significant. After eliminating insignificant factors (if the quadratic term of a factor is significant, the model must retain its primary term), quadratic regression models were developed between the test factors and quality of feed index and miss index, as shown in Equations (16) and (17).

$$y_1 = -42.52 + 18.81x_1 + 2.22x_2 + 1.61x_3 - 5.79x_1^2 - 0.01x_2^2 - 0.07x_3^2,\ R^2 = 0.89 \quad (16)$$

$$y_2 = 25.01 - 21.80x_1 + 6.42x_1^2,\ R^2 = 0.79 \quad (17)$$

a. Disc b. Air chamber

Figure 16 Internal structure of the seed meter after 4 hours of operation

Table 3 Box-Behnken test results

Test No.	x_1	x_2	x_3	y_1	y_2	y_3
1	0	1	–1	87.96	6.57	5.46
2	1	0	1	85.28	11.20	3.54
3	–1	–1	0	80.65	16.94	2.41
4	1	0	–1	83.89	11.02	5.09
5	1	–1	0	85.65	10.74	3.62
6	0	0	0	88.24	6.85	4.91
7	0	1	1	83.61	12.22	4.17
8	–1	0	1	80.93	14.26	4.82
9	0	0	0	90.83	7.41	1.76
10	0	0	0	91.76	5.74	2.50
11	1	1	0	82.22	9.54	8.24
12	–1	0	–1	81.48	16.02	2.50
13	0	–1	–1	86.67	6.39	6.94
14	0	0	0	92.96	3.80	3.28
15	0	–1	1	86.39	6.94	6.67
16	–1	1	0	82.50	15.65	1.85
17	0	0	0	91.57	3.43	5.00

Note: x_1, x_2, and x_3 are the coded values of the height of the seed disturbance structure, upper arc diameter, and upper arc central angle, respectively. y_1, y_2, and y_3 are the quality of feed index, miss index, and multiple index of Wuyou 1179, respectively.

The optimal parameters are obtained to maximize the quality of feed index and minimize the miss index. The optimal parameters of the seed disturbance structure were obtained as follows: the height of the seed disturbance structure is 1.65 mm, the diameter of the upper arc is 98.87 mm, and the central angle of the upper arc is 11.4°. The predicted quality of feed index is 91.20%, and the predicted miss index is 6.51%. The seed disturbance structure is manufactured according to the optimal parameters, and validation tests are performed. The quality of feed index and miss index of the seed meter with the optimal seed disturbance structure are 90.28%

and 5.28%, which is less error than the predicted test results, proving that the model is regression reliable.

3.3 Shaped hole structure parameters

3.3.1 Experiment

When the rotational speed was 20 r/min, the quality of feed index was 6 mm width, 5 mm width, 3 mm width, and 4 mm width in ascending order over the vacuum range of 1.6-3.2 kPa (Figure 17a). At 40 r/min, the quality of feed index was lowest for a 6 mm width and highest for a 4 mm width in the vacuum range of 1.6-3.2 kPa (Figure 17b). At 60 r/min, the quality of feed index was 6 mm width, 5 mm width, 3 mm width, and 4 mm width in ascending order over the vacuum range of 1.6-2.8 kPa (Figure 17c). The main reason the pass rate of 4 mm width is optimal is that the width of 4 mm prevents too many seeds from entering the shaped hole and ensures that the seeds enter the shaped hole quickly. When the vacuum pressure is 2.0-3.2 kPa, the quality of feed index at high speed is higher than that at low speed, and the quality of feed index of width 3 mm and width 4 mm is especially obvious. This is mainly because the short filling time at high speeds reduces the occurrence of multiple seeds being suctioned by a single hole.

Table 4 ANOVA of regression model

Source	Quality of feed index				Miss index			
	Sum of squares	d_f	F-value	p-value	Sum of squares	d_f	F-value	p-value
Model	241.05	9	11.28	0.0021**	253.62	9	6.35	0.0117*
x_1	16.48	1	6.94	0.0337*	51.87	1	11.7	0.0111*
x_2	1.17	1	0.49	0.5059	2.41	1	0.543	0.4852
x_3	1.8	1	0.76	0.4126	1.28	1	0.2893	0.6073
x_1x_3	6.96	1	2.93	0.1305	0.0021	1	0.0005	0.9831
x_1x_2	0.95	1	0.40	0.5481	0.9452	1	0.2131	0.6583
x_2x_3	4.15	1	1.75	0.2278	3.36	1	0.7579	0.4128
x_1^2	141.24	1	59.47	0.0001**	164.72	1	37.14	0.0005**
x_2^2	26.90	1	11.33	0.012*	9.71	1	2.19	0.1825
x_3^2	24.03	1	10.12	0.0155*	8.56	1	1.93	0.2073
Residual	16.62	7			31.04	7		
Lack of fit	4.25	3	0.46	0.73	18.33	3	1.92	0.2675
Pure error	12.37	4			12.71	4		
Total	257.67	16			284.66	16		

Note: * indicates significant ($0.01<p<0.05$) and ** indicates highly significant ($p<0.01$).

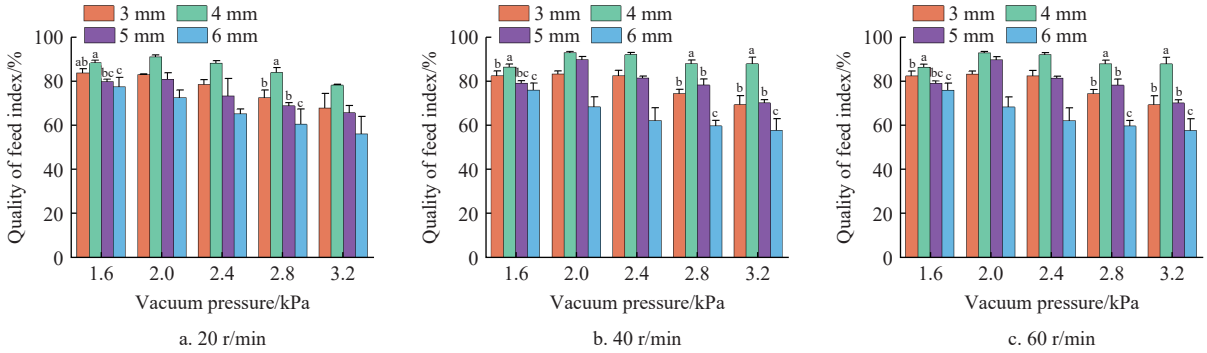

a. 20 r/min b. 40 r/min c. 60 r/min

Note: Different lowercase letters indicate significant differences ($p<0.05$).

Figure 17 Quality of feed index at 20 r/min, 40 r/min, and 60 r/min for different shaped hole widths

As shown in Figure 18, the miss index decreases with increasing vacuum pressure for different hole widths when the speeds are 20 r/min, 40 r/min, and 60 r/min. This is mainly because as the vacuum increases, the suction force of the seed meter increases, which can reduce the occurrence of misses. At a speed of 20 r/min and a vacuum pressure of ≥2 kPa, the miss index was less than 5% for various widths (Figure 18a). At a speed of 40 r/min and a vacuum of ≥2.4 kPa, the miss index of the seed was less than 4% for the different widths (Figure 18b). However, when the speed was 60 r/min, the miss index of the 3 mm-width seed was higher than the other widths at vacuum pressures of 1.6-2.8 kPa (Figure 18c). This is due to the short duration of the seed-filling process at 60 r/min, which makes it difficult for the seeds to fill the 3 mm-wide hole. At vacuum pressures ≥ 2 kPa, the differences in miss index between the 4 mm, 5 mm, and 6 mm widths were small.

At a rotational speed of 20 r/min and a vacuum pressure ≥2 kPa, the multiple index of different widths were 4 mm, 3 mm, 5 mm, and 6 mm in ascending order (Figure 19a). At a rotational speed of 40 r/min and a vacuum pressure ≥2 kPa, the multiple index of different widths were 4 mm, 5 mm, 3 mm, and 6 mm in ascending order (Figure 19b). At a speed of 60 r/min and a vacuum pressure ≥2 kPa, the multiple index was higher for the 6 mm and 5 mm widths than for the 4 mm and 3 mm widths (Figure 19c). Seeds are more likely to go into the wider type holes, which hold more seeds when filled (Figure 20c and Figure 20d). A 4 mm width will allow the seed to remain stable in the hole (Figure 20b). When the vacuum was ≥2 kPa, and the speeds were 20 r/min and 40 r/min, the multiple index of the 3 mm hole width was much greater than that of the 4 mm hole width. However, at vacuum pressure ≥ 2 kPa and a speed of 60 r/min, there was little difference in multiple index between a 4 mm width and a 3 mm width. The filling time is long at low speeds, and the suction holes are easily filled with seed. Because the suction hole width of 3 mm is too small, it is difficult for seeds to enter the hole to maintain a stable seed-filling position. Multiple seeds are suctioned by the same hole to form an agglomerate (Figure 20a), resulting in a higher multiple index for a 3 mm hole width than a 4 mm hole width. As the speed increases, the seed-filling time decreases, and the probability of multiple seeds being suctioned in the 3 mm hole width decreases, so there is not much difference in multiple index between the 3 mm width and the 4 mm width at high speeds.

3.3.2 CFD-DEM numerical simulations

At the end of the simulation, the drag and pressure gradient forces on the suctioned seeds of different shaped holes were counted, and a total of 10 groups of holes were counted. The drag and pressure gradient forces on the seed in the flow field are shown in Figure 21, and the seed meter filling is shown in Figure 22. The seed is subjected to a pressure gradient force greater than the trailing force. The pressure gradient and drag forces are 3 mm, 4 mm, 5 mm, and 6 mm in descending order. The main reason for this phenomenon is that the smaller the opening width, the greater the air velocity around the seed.

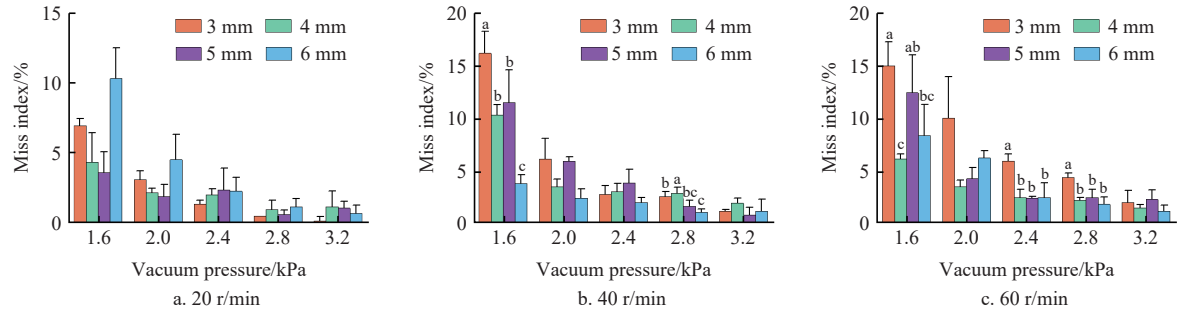

Note: Different lowercase letters indicate significant differences (p<0.05).

Figure 18 Miss index at 20 r/min, 40 r/min, and 60 r/min for different shaped hole widths

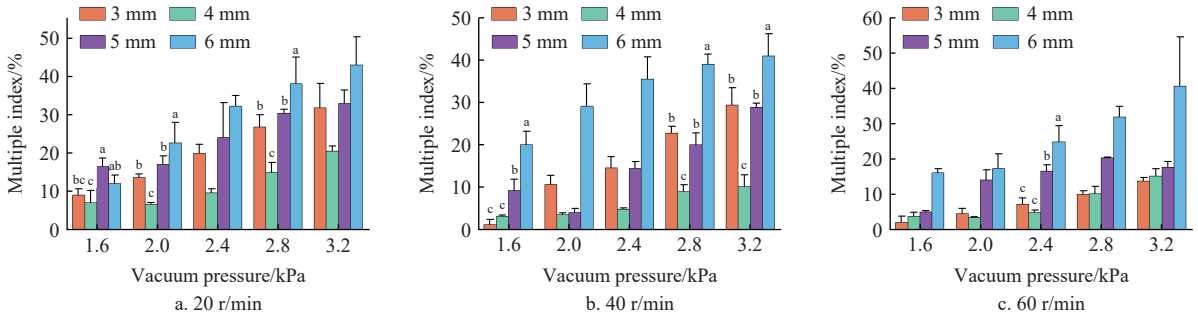

Note: Different lowercase letters indicate significant differences (p<0.05).

Figure 19 Multiple index at 20 r/min, 40 r/min, and 60 r/min for different shaped hole widths

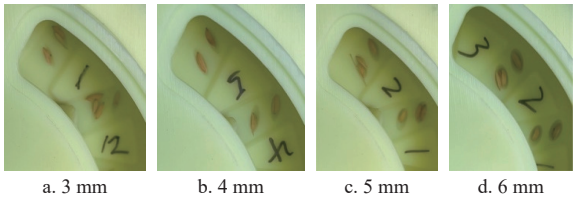

Figure 20 Seed filling with different shaped hole widths at 40 r/min and 2.4 kPa vacuum

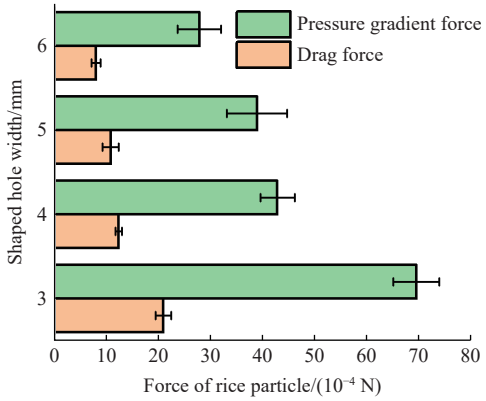

Figure 21 Forces on rice seed in CFD-DEM coupling

In conclusion, the optimal shaped hole structure parameters are 4 mm hole width and 2 mm hole depth. When the rotational speed was 20 r/min, and the vacuum pressure was 2.0 kPa and 2.4 kPa, for the optimal shaped hole structure, the miss index was 2.22% and 2.04%; the quality of feed index was 90.74% and 87.96%; and the multiple index was 7.04% and 10.00%, respectively. When the rotational speed was 40 r/min, and the vacuum pressure was 2.0 kPa, 2.4 kPa, 2.8 kPa, and 3.2 kPa, for the optimal hole structure, the miss index was 3.52%, 3.06%, 2.87%, and 1.94%; the quality of feed index was 92.5%, 91.67%, 87.69%, and 87.5%; and the multiple index was 3.98%, 5.28%, 9.44% and 10.56%, respectively. When the rotational speed was 60 r/min, and the vacuum pressure was 2.0 kPa to 2.8 kPa, for the optimal shaped hole structure, the miss index was 3.52%, 2.5%, and 2.22%; the quality of feed index was 92.41%, 92.13%, and 87.13%; and the multiple index was 4.07%, 5.37%, and 10.65%, respectively. The planting accuracy of the optimal hole can meet the agronomic requirements for direct seeding of rice in the field.

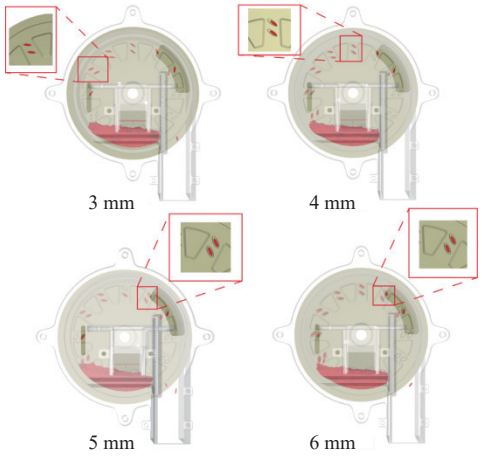

Figure 22 Filling seed of different shaped holes in CFD-DEM coupling

3.4 Planting accuracy of different rice seeds

In order to verify the optimal parameters of the seed meter, experiments were carried out to obtain the miss index (MISS), quality of feed index (QFI), and multiple index (MULT) of Huanghuazhan and Taixiang 812; results are listed in Table 5. When the rotational speed was 60 r/min, and the vacuum pressure was 1.6 kPa, 1.8 kPa, 2.0 kPa, and 2.2 kPa, for Huanghuazhan, the miss index was 2.5%, 0.74%, 1.11 %, and 1.20%; the quality of feed was 87.59%, 91.67%, 90.83%, and 85.56%; and the multiple index was 9.91%, 7.59%, 8.06%, and 13.24%, respectively. For Taixiang 812 rice seed, when the rotational speed was 60 r/min, and

the vacuum pressure was 2.4 kPa, 2.6 kPa, and 2.8 kPa, the miss index was 4.44%, 3.43%, and 2.41%; the quality of feed was 81.85%, 80.65%, and 79.35%; and the multiple index was 13.70%, 15.93%, and 18.24%, respectively.

Table 5 Planting accuracy of Huanghuazhan and Taixiang 812

Rotational speed/ r·min^{-1}	Vacuum pressure/ kPa	Huanghuazhan			Taixiang 812		
		MISS/%	QFI/%	MULT/%	MISS/%	QFI/%	MULT/%
20	1.6	2.87	81.30	15.83	6.20	81.48	12.31
	1.8	2.41	82.69	14.91	4.17	82.41	13.43
	2.0	0.56	78.98	20.46	6.02	79.35	14.63
	2.2	0.56	80.09	19.35	1.85	79.26	18.89
	2.4	0.09	79.72	20.19	2.22	75.56	22.22
	2.6	0.00	77.87	22.13	2.13	76.39	21.48
	2.8	0.09	66.67	33.24	2.13	75.65	22.22
40	1.6	6.39	85.09	8.52	9.26	82.31	8.43
	1.8	2.31	88.61	9.07	5.28	81.02	13.70
	2.0	2.96	87.50	9.54	4.54	76.85	18.61
	2.2	0.65	86.67	12.69	5.00	77.22	17.78
	2.4	1.76	83.06	15.19	4.81	75.74	19.44
	2.6	0.37	81.02	18.61	2.87	77.69	19.44
	2.8	1.11	74.81	24.07	1.76	73.70	24.54
60	1.6	2.50	87.59	9.91	8.24	86.30	5.46
	1.8	0.74	91.67	7.59	7.78	79.81	12.41
	2.0	1.11	90.83	8.06	7.04	82.96	10.00
	2.2	1.20	85.56	13.24	6.48	79.44	14.07
	2.4	1.94	83.52	14.54	4.44	81.85	13.70
	2.6	1.57	78.24	20.19	3.43	80.65	15.93
	2.8	1.57	78.52	19.91	2.41	79.35	18.24

It is clear that the planting accuracy of Huanghuazhan is better than that of Taixiang 812. The width and thickness of the Taixiang 812 seed are smaller than those of the Huanghuazhan seed, but the length is greater than that of the Huanghuazhan. At the same vacuum pressure and rotational speed, the suction force of Taixiang 812 seed is smaller than that of Huanghuazhan seed because the windward area of Taixiang 812 is smaller than that of Huanghuazhan. This also explains the higher miss index of Taixiang 812 seeds as compared to Huanghuazhan. For direct seeding of rice in paddy fields, the seed meter should ensure a low miss index, and a high multiple index is acceptable. With the right vacuum pressure, Huanghuazhan and Taixiang 812 will have a low miss index, which satisfies the planting accuracy for rice direct seeding.

4 Conclusions

1) The key components of the vacuum seed meter with the double hole for rice were designed. The number of holes was determined to be 12, the diameter of the holes was determined to be 1.6 mm, and the location of the holes was determined. The design of the anti-clogging device, the seed disturbance structure, and the shaped hole were carried out, and the spring parameters of the anti-clogging device were determined.

2) Regression models of quality of feed index and miss index for Wuyou 1179 rice seed were established. The optimal parameters of the seed disturbance structure were obtained as a height of the seed disturbance structure of 1.65 mm, a diameter of the upper arc of 98.87 mm, and a central angle of the upper arc of 11.4°. Validation experiments showed that the regression model is reliable when the vacuum and speed are 2.0 kPa and 40 r/min, respectively.

3) The width of the shaped hole affected the planting accuracy of Wuyou 1179. At a speed of 60 r/min, the miss index was higher for a 3 mm width than for the other widths. The lowest miss index was observed at 20 and 40 r/min with vacuum ≥2 kPa for a 4 mm width. The pressure gradient force on the seed is greater than the drag force, and the pressure gradient force and drag force are positively correlated with the shaped hole width. The test results show that the optimal hole structure parameters are 4 mm hole width and 2 mm hole depth.

Acknowledgements

This work was financially supported by the Guangdong Province Key Field Research and Development Program (Grant No. 2023B0202130001), the National Natural Science Foundation of China (Grant No. 52175228), Guangdong Basic and Applied Basic Research Foundation (Grant No. 2020A1515110225), China Agriculture Research System for rice (CARS-01), and the Laboratory of Lingnan Modern Agriculture Project (Grant No. NT2021009).

[References]

[1] Ren D Y, Ding C Q, Qian Q. Molecular bases of rice grain size and quality for optimized productivity. Science Bulletin, 2023; 68(3): 314–350.

[2] Xing H, Wang Z M, Luo X W, Zang Y, He S Y, Xu P, et al. Design and experimental analysis of rice pneumatic seeder with adjustable seeding rate. Int J Agric & Bio Eng, 2021; 14(4): 113–122.

[3] Zhang M H, Wang Z M, Luo X W, Zang Y, Yang W W, Xing H, et al. Review of precision rice hill-drop drilling technology and machine for paddy. Int J Agric & Bio Eng, 2018; 11(3): 1–11.

[4] Li H Q, Zhao C J, Yan B X, Ling L, Meng Z J. Design and verification of the variable capacity roller-wheel precision rice direct seed-metering device. Agronomy-Basel, 2022; 12(8): 1798.

[5] Li X Z, Dong J F, Zhu W, Zhao J L, Zhou L Y. Progress in the study of functional genes related to direct seeding of rice. Molecular Breeding, 2023; 43(6): 46.

[6] Kumar S, Verma S K, Yadav A, Taria S, Alam B, Banjara T R. Tillage based crop establishment methods and zinc application enhances productivity, grain quality, profitability and energetics of direct-seeded rice in potentially zinc-deficient soil in the subtropical conditions of india. Communications in Soil Science and Plant Analysis, 2022; 53(9): 1085–1099.

[7] Tao Y, Chen Q, Peng S B, Wang W Q, Nie L X. Lower global warming potential and higher yield of wet direct-seeded rice in central China. Agronomy for Sustainable Development, 2016; 36(2): 24.

[8] Liu H Y, Hussain S, Zheng M M, Peng S B, Huang J L, Cui K H, et al. Dry direct-seeded rice as an alternative to transplanted-flooded rice in central china. Agronomy for Sustainable Development, 2015; 35(1): 285–294.

[9] Fu W, Zhang Z Y, Zang Y, Luo X W, Zeng S, Wang Z M. Development and experiment of rice hill-drop drilling machine for dry land based on proportional speed regulation. Int J Agric & Bio Eng, 2017; 10(4): 77–86.

[10] Li H, Zeng S, Luo X W, Fang L Y, Liang Z H, Yang W W. Design, dem simulation, and field experiments of a novel precision seeder for dry direct-seeded rice with film mulching. Agriculture-Basel, 2021; 11(5): 378.

[11] Li H Q, Yan B X, Meng Z J, Ling L, Yin Y X, Zhang A Q, et al. Study on influencing factors of hole-filling performance of rice precision direct seed-metering device with hole ejection. Biosystems Engineering, 2023; 233: 76–92.

[12] He S Y, Qian C, Jiang Y C, Qin W, Huang Z S, Huang D M, et al. Design and optimization of the seed feeding device with DEM-CFD coupling approach for rice and wheat. Computers and Electronics in Agriculture, 2024; 219: 108814.

[13] Qian C, He S Y, Qin W, Jiang Y C, Huang Z S, Zhang M L, et al. Influence of shaped hole and seed disturbance on the precision of bunch planting with the double-hole rice vacuum seed meter. Agronomy-Basel, 2024; 14(4): 768.

[14] Ding L, Yuan Y C, Dou Y F, Li C X, He Z, Guo G M, et al. Design and experiment of air-suction maize seed-metering device with auxiliary guide. Agriculture-Basel, 2024; 14(2): 169.

[15] Wang Z Y, Su W, Lai Q H, Li J H, Gao X J. Boundary modelling of the

effective suction domain of an air-suction seed-metering device for quasi-spherical seeds. Biosystems Engineering, 2024; 238: 212–226.

[16] Ignaciuk S, Zarajczyk J, Rózanska-Boczula M, Borusiewicz A, Kubon M, Barta D, et al. Predicting the seeding quality of radish seeds with the use of a family of nakagami distribution functions. International Agrophysics, 2024; 38(1): 21–29.

[17] St Jack D, Hesterman D C, Guzzomi A L. Precision metering of santalum spicatum (australian sandalwood) seeds. Biosystems Engineering, 2013; 115(2): 171–183.

[18] Du X, Liu C L. Design and testing of the filling-plate of inner- filling positive pressure high-speed seed-metering device for maize. Biosystems Engineering, 2023; 228: 1–17.

[19] Tang H, Xu F D, Guan T Y, Xu C S, Wang J W. Design and test of a pneumatic type of high-speed maize precision seed metering device. Computers and Electronics in Agriculture, 2023; 211: 107997.

[20] Tang H, Guan T, Xu F, Xu C, Wang J. Test on adsorption posture and seeding performance of the high-speed precision dual-chamber maize metering device based on the seed characteristics. Computers and Electronics in Agriculture, 2024; 216: 108471.

[21] Zhao P, Gao X, Su Y, Xu Y, Huang Y. Investigation of seeding performance of a novel high-speed precision seed metering device based on numerical simulation and high-speed camera. Computers and Electronics in Agriculture, 2024; 217: 108563.

[22] Li C, Cui T, Zhang D X, Yang L, He X T, Li Z M, et al. Design and experiment of a centrifugal filling and cleaning high-speed precision seed metering device for maize. Journal of Cleaner Production, 2023; 426: 139083.

[23] Zhao X, Zhang T, Liu F, Li N, Li J R. Sunflower seed suction stability regulation and seeding performance experiments. Agronomy-Basel, 2023; 13(1): 54.

[24] Degirmencioglu A, Çakmak B, Yazgi A. Prototype twin vacuum disk metering unit for improved seed spacing uniformity performance at high forward speeds. Turkish Journal of Agriculture and Forestry, 2018; 42(3): 195–206.

[25] Yazgi A, Degirmencioglu A. Measurement of seed spacing uniformity performance of a precision metering unit as function of the number of holes on vacuum plate. Measurement, 2014; 56: 128–135.

[26] Pareek C M, Tewari V K, Machavaram R. Multi-objective optimization of seeding performance of a pneumatic precision seed metering device using integrated ann-mopso approach. Engineering Applications of Artificial Intelligence, 2023; 117: 105559.

[27] Karayel D, Güngör O, Sarauskis E. Estimation of optimum vacuum pressure of air-suction seed-metering device of precision seeders using artificial neural network models. Agronomy-Basel, 2022; 12(7): 1600.

[28] Markauskas D, Platzk S, Kruggel-Emden H. Comparative numerical study of pneumatic conveying of flexible elongated particles through a pipe bend by DEM-CFD. Powder Technology, 2022; 399: 117170.

[29] Mori Y, Sakai M. Development of a robust Eulerian-Lagrangian model for the simulation of an industrial solid-fluid system. Chemical Engineering Journal, 2021; 406: 126841.

[30] Zou J X, Zhang R, Zhou F Y, Zhang X Q. Hazardous area reconstruction and law analysis of coal spontaneous combustion and gas coupling disasters in goaf based on DEM-CFD. Acs Omega, 2023; 8(2): 2685–2697.

[31] Xu J, Sun S L, He Z K, Wang X M, Zeng Z H, Li J, et al. Design and optimisation of seed-metering plate of air-suction vegetable seed-metering device based on DEM-CFD. Biosystems Engineering, 2023; 230: 277–300.

[32] Mudarisov S, Badretdinov I, Rakhimov Z, Lukmanov R, Nurullin E. Numerical simulation of two-phase "air-seed" flow in the distribution system of the grain seeder. Computers and Electronics in Agriculture, 2020; 168: 105151.